THE JOURNAL OF COMPARATIVE NEUROLOGY 470:164–180 (2004)

Electron Microscopy of Degenerative Changes in the Chick Basilar Papilla after Gentamicin Exposure

KEIKO HIROSE,[1] LESNICK E. WESTRUM,[2,3] DALE E. CUNNINGHAM,[2] AND EDWIN W RUBEL[1–3]*

[1]Department of Otolaryngology-Head and Neck Surgery, University of Washington, Seattle, Washington 98195

[2]Virginia Merrill Bloedel Hearing Research Center, University of Washington, Seattle, Washington 98195

[3]Department of Neurological Surgery, University of Washington, Seattle, Washington 98195

ABSTRACT

We present a sequential study of the substructural alterations in the chick basilar papilla at the earliest signs of hair cell degeneration. Three-day posthatch chicks received a single injection of gentamicin (300 mg/kg) and were killed at 6, 8, 12, 15, 18, 21, and 24 hours after the injection. The basilar papillae were studied by conventional transmission electron microscopy. Examination was limited to the basal region, where all hair cells are eliminated by this treatment. As early as 8 hours and clearly by 12 hours, altered fine structure was seen in hair cells. Changes included rounding and swelling of the hair cells, condensation of nuclear chromatin, dissolution of ribosomes, dilatation of the mitochondria, and accumulation of inclusion bodies and lysosomes. By 15–18 hours, lysosomes increased and became denser, afferent terminals appeared swollen, and the first cell extrusion was seen. Efferents were unaffected, and supporting cells, though having inclusion bodies now, retained normal intercellular junctions. By 21–24 hours, large regions of complete hair cell loss were composed of expanded supporting cell processes with normal-appearing intercellular junctions and portions of extruded hair cells, partially attached to the supporting cell surface. These observations demonstrate that auditory hair cells undergo a rapid and controlled process of hair cell extrusion that allows preservation of the reticular lamina and minimal contamination of surrounding structures by intracytoplasmic contents of the damaged hair cells. J. Comp. Neurol. 470:164–180, 2004.

Indexing terms: ototoxicity; hearing loss; inner ear; cochlea

Aminoglycoside antibiotics are ototoxic agents that are responsible for significant morbidity because of their vestibulotoxic and cochleotoxic effects. Although studies dating back to 1962 have demonstrated various characteristic changes in the sensory epithelium of the inner ear after aminoglycoside exposure, a systematic study of the earliest changes leading to the extrusion of hair cells has not yet been performed. Various protocols for drug exposure and numerous animal species have been studied to elucidate the anatomic and morphologic processes, the physiologic changes, and the cellular mechanisms involved in ototoxic hair cell death. Nonetheless, the mechanisms involved in hair cell death remain elusive (Forge and Li, 2000).

The chick has become a very popular species in which to study cellular changes after aminoglycoside exposure because of its capacity to regenerate hair cells (Cotanche et al., 1987; Cruz et al., 1987; Stone et al., 1996). In an attempt to improve our understanding of the events lead-

Grant sponsor: National Institute on Deafness and Other Communication Disorders; Grant number: DC04661; Grant number: DC02854; Grant sponsor: Oberkotter Foundation.

Keiko Hirose's current address is Departments of Neurosciences and of Otolaryngology and Communicative Disorders, Cleveland Clinic Foundation, 9500 Euclid Avenue, Cleveland, OH 44195.

*Correspondence to: Edwin W Rubel, Department of Otolaryngology-Head and Neck Surgery, University of Washington, Seattle, WA 98195. E-mail: rubel@u.washington.edu

Received 9 May 2003; Revised 16 September 2003; Accepted 27 October 2003

DOI 10.1002/cne.11046

Published online the week of January 19, 2004 in Wiley InterScience (www.interscience.wiley.com).

ing to hair cell regeneration, we undertook a detailed longitudinal study of the process of hair cell degeneration preceding the early events of regeneration. The specific cytologic events that take place prior to regeneration may influence the success of the regeneration process and may therefore help to elucidate the absence of hair cell regeneration in the mammalian inner ear.

Although many papers include detailed observations of anatomic changes after chronic aminoglycoside-induced ototoxicity in birds and mammals (for reviews see Cotanche, 1999; Forge and Schacht, 2000; Ryan, 2002; Raphael, 2002), descriptions of the acute degenerative changes are difficult to find. At least two methodological conditions in most previous experiments have complicated such observations; repeated drug exposures and long survival times. Most of the studies to date have used chronic drug exposure, taking several days, coupled with survival times of days to weeks following the final treatment. Thus, a description of the earliest cellular alterations preceding hair cell death is not available in these studies. In addition, in birds and reptiles, degeneration, proliferation, and differentiation of new cells are likely to be occurring over the same time interval when a multiple-treatment paradigm is used. Finally, when there are diverse populations of hair cells reacting differently to a chronic exposure of a toxic agent, it is difficult to discern early changes in the cells that ultimately degenerate vs. changes in cells that ultimately survive. These confounding factors have been overcome in the present study by 1) use of a single injection of an aminoglycoside known to cause complete hair cell loss at the basal one-third of the basilar papilla (Bhave et al., 1995; Janas et al., 1995) and 2) very early and closely spaced survival times.

The inner ears of mammals such as guinea pigs, gerbils, and chinchillas have been carefully studied by using ultrastructural methods after multiple injections over 7–14 days, with the earliest survival at 2–3 days after the last exposure (Anniko et al., 1982; Chen and Saunders, 1983; Gratacap et al., 1985; Hayashida et al., 1985; McDowell et al., 1989; Kotecha and Richardson, 1994; Leake et al., 1997). Two groups, however, have addressed some of the early changes after ototoxic exposure in the mammalian ear. Hayashida and colleagues (1989) studied guinea pig cochlea and vestibular organs from 3 to 48 hours after radiolabeled aminoglycoside exposure. In this case, the authors combined the aminoglycoside with noise exposure. De Groot and coworkers (1990, 1991) described changes as early as 24 hours after the last injection, but they used 5–15 days of daily injections. These studies nevertheless did identify types of cytoplasmic organelles affected and proposed possible cytologic pathways for aminoglycoside-induced hair cell changes.

Cellular studies of hair cell ototoxicity in postnatal birds are fewer than those of the mammalian inner ear (Umemoto et al., 1994; Cotanche et al., 1994; Epstein and Cotanche, 1995; Hashino and Shero, 1995; Hashino et al., 1997) and with few exceptions also used multiple injections and longer survivals of several days to weeks. Hashino and Shero (1995) and Hashino et al. (1997) describe the use of radiolabeled aminoglycoside to determine the pathway of antibiotic molecules into and through lysosomes of hair cells and used a single dose paradigm with short survival times (3–27 hours). However, these studies did not describe other ultrastructural changes within the hair cell that may be pertinent to ototoxic mechanisms. In addition, a series of papers has used a single-treatment aminoglycoside paradigm to study hair cell regeneration (see, e.g., Bhave et al., 1995; Janas et al., 1995; Stone et al., 1996; Torchinsky et al., 1999; Roberson et al., 2000).

This report provides a detailed ultrastructural description of the morphological events and subcellular changes occurring within the chick auditory hair cells at closely spaced time intervals immediately following a single injection of gentamicin. The findings provide a sequence that leads to death and hair cell extrusion and the possible involvement of the supporting cells in this process. We have studied the chick not only because of its capacity to regenerate new hair cells but because several culture preparations of the basilar papillae have been developed that can be used to address more specific questions regarding mechanisms (Oesterle et al., 1993; Stone et al., 1996; Hirose et al., 1997, 1999; Matsui et al., 2002; Cheng et al., 2003). Preliminary reports of this study have been presented previously (Westrum et al., 1998; Hirose et al., 1999).

MATERIALS AND METHODS

Degenerative changes in hair cells and supporting cells were examined in the chick basilar papilla, by using conventional transmission electron microscopy (TEM). White leghorn chicks (*Gallus domesticus*) at posthatch days 3–5 were injected subcutaneously with a single dose (300 mg/kg) of gentamicin sulfate (Sigma, St. Louis, MO). Details of animal care conformed to standards established by the NIH and the University of Washington Institutional Animal Care and Use Committee (IACUC).

Emphasis is directed to the ultrastructural changes during the first 24 hours after the single injection. Survival times of 6, 8, 12, 15, 18, 21, and 24 hours were chosen. At minimum three chicks (six basilar papillae) were studied at each time point along with age-matched broodmates as controls. The chicks were quickly decapitated, and the oval window was exposed by removal of the columella. The otic capsule was opened in the distal part of the basilar papilla by using sharp dissection. Inner ears were then sequentially fixed bilaterally by an intralabyrinthine perfusion of a cold mixture of 2% paraformaldehyde and 2.5% glutaraldehyde in 0.1 M sodium cacodylate buffer at pH 7.4 for 3–4 minutes. The time lapse from the start of dissection to perfusion of fixation was usually no more than 2–3 minutes. After perfusion, basilar papillae were exposed, and the entire head was immersed in the same fixative for 1 hour on a shaker table and then overnight at 4°C. On the following day, heads were rinsed three times in 0.1 M cacodylate buffer, and the papillae were dissected free of the temporal bones. Basilar papillae were then postfixed in 1% OsO_4 in the same buffer for 1 hour at 4°C. The specimens were then rinsed in buffer (3×10 minutes), dehydrated through graded ethanolic solutions, infiltrated via propylene oxide (Aldrich Chemical Co., Milwaukee, WI), and embedded in Spurr's epoxy resin (Ted Pella, Inc., Redding, CA). En bloc staining with saturated alcoholic uranyl acetate was carried out on some of the specimens during the dehydration steps.

The area of the papilla 400 μm (±25 μm) from the proximal (basal) tip was selected as the area of study. This region is within the area that consistently undergoes complete hair cell loss from a single in vivo gentamicin exposure at this dosage (Janas et al., 1995; Stone et al., 1996;

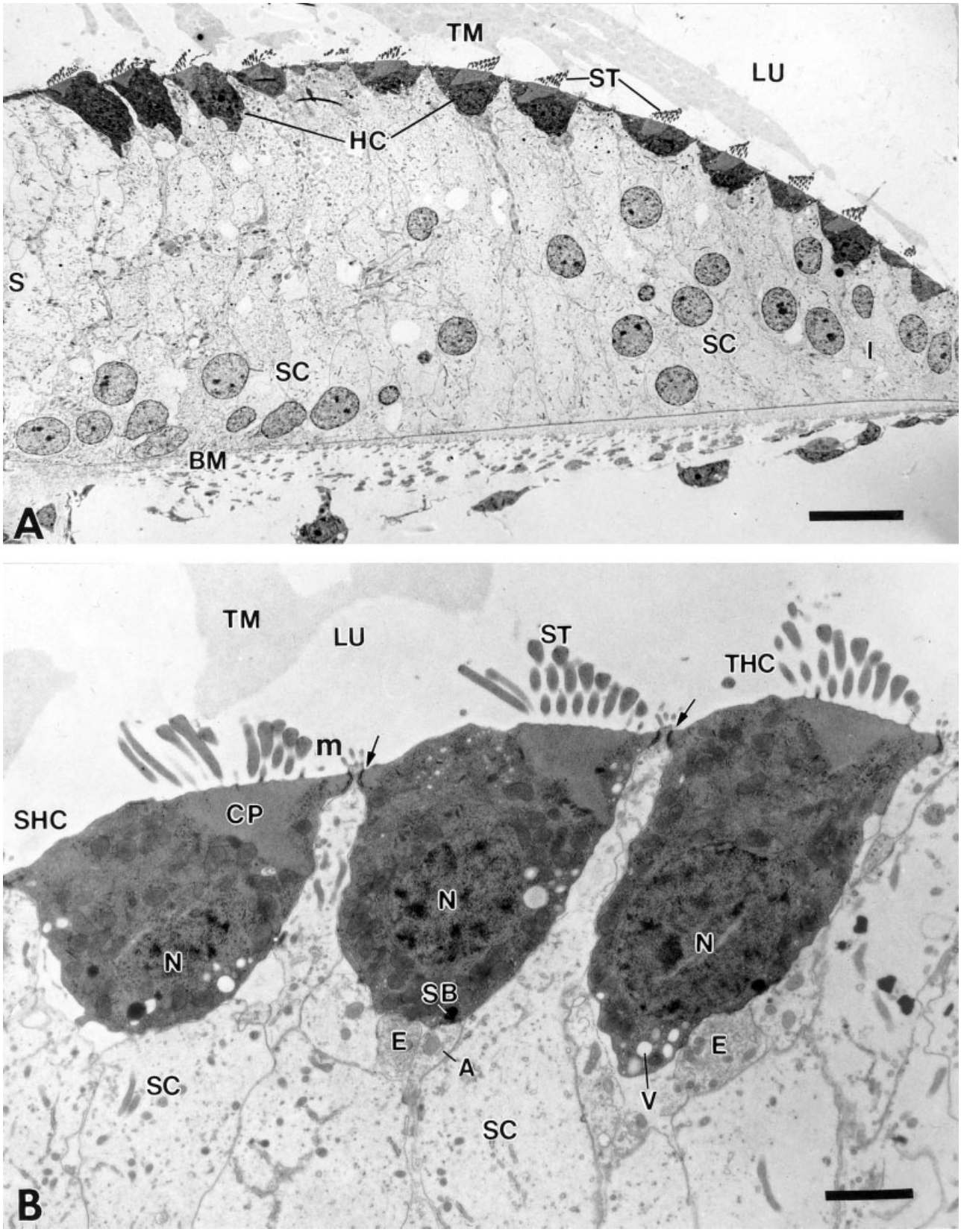

Fig. 1. **A:** Electron micrograph of a transverse section through the basilar papilla of a normal posthatch day 4 chick, taken at approximately 400 μm from the basal tip. Hair cells (HC) with bundles of stereocilia (ST) occur at the lumen (LU), and the nuclei of the organ supporting cells (SC) are seen along the basilar membrane (BM) or scattered at the abneural or inferior region (I). The superior region (S) is to the left and the tectorial membrane (TM) above. **B:** Higher magnification of short (SHC) and intermediate or taller (THC) hair cells from a normal basilar papilla at the same level as in A. Bundles of stereocilia (ST), vacuoles (V), cuticular plates (CP), and nuclei (N) are seen as are interspersed organ supporting cell (SC) processes with their microvilli (m) and specialized junctions (arrows) between themselves and the hair cells (also see subsequent figures). Efferent (E) and afferent (A) neural terminals contact the basal portion of the hair cells. A synaptic body (SB) is seen in the hair cell apposed to the afferent terminal. Scale bars = 10 μm in A, 2 μm in B.

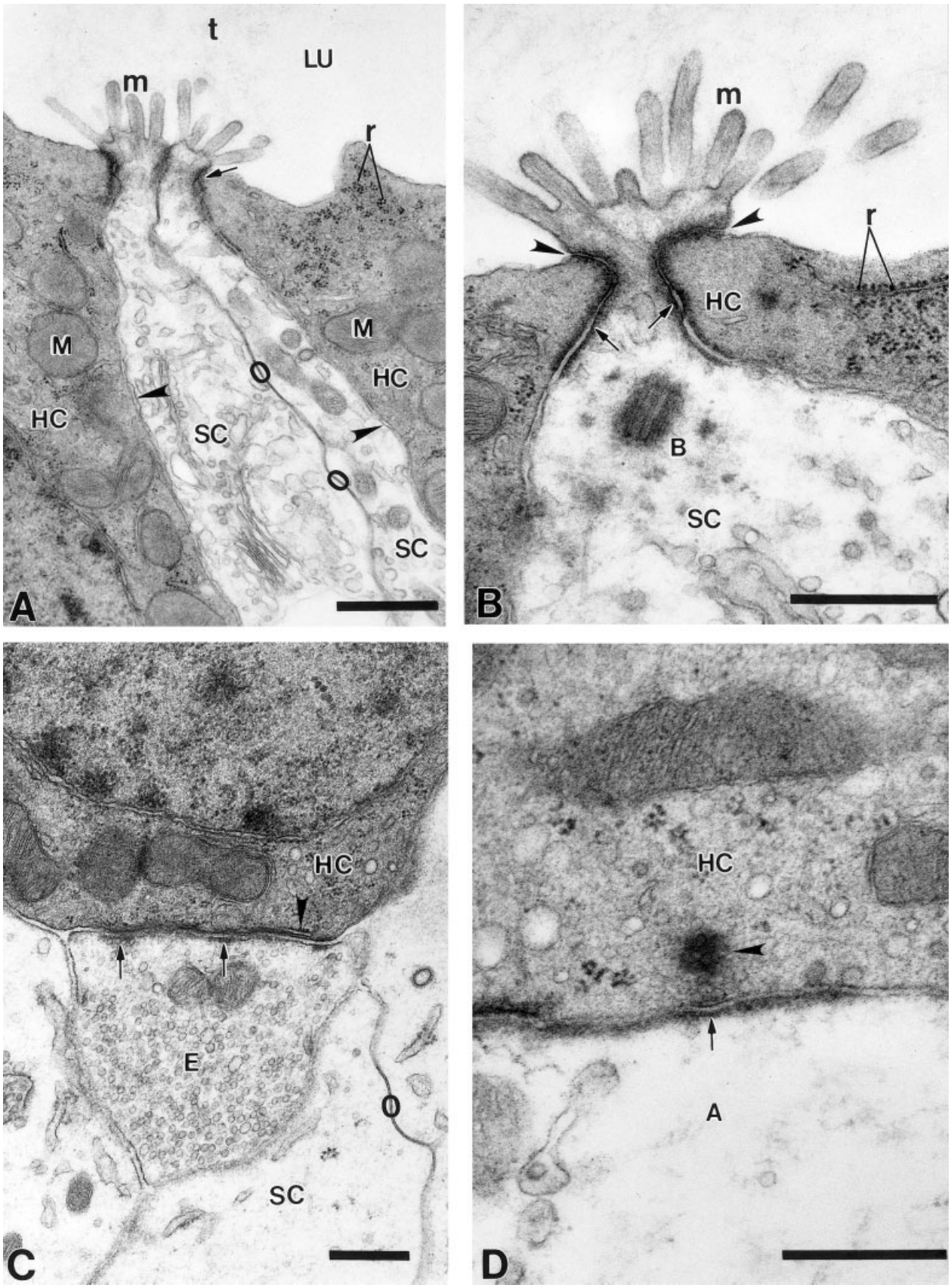

Figure 2

Roberson et al., 2000). Consecutive semithin sections (1 μm) were collected, stained with toluidine blue, and examined until the most basal aspect of the sensory epithelium could be identified. Then, at each 50-μm interval, several 1-μm sections were collected, stained, and examined to verify the proximal-distal level and also to evaluate cytologic features. If the location and the quality of the tissue were acceptable, the block was used for ultrathin sectioning and TEM analysis.

Ultrathin sections (90 nm) in the transverse plane were then serially collected on formvar- and carbon-coated, slotted or mesh copper grids. At minimum five consecutive grids were obtained from each block/papilla for study. The grids were stained with uranyl acetate and lead citrate and viewed with a Philips EM LS 410 transmission electron microscope. A photomicrography routine was performed on consecutive sections from each papilla as follows: 1) survey full-frame, single pictures were taken of the entire sensory epithelium at about ×800; 2) higher magnification, overlapping negatives were obtained across the papilla at ×3,000–6,000; and, finally, 3) selected areas of interest, as determined by findings in the lower and midrange photographs, were photographed at increased magnifications of ×10,000 to ×25,000 in order to evaluate specific ultrastructural features. At least 24 negatives were obtained for each sampled region, and at least 72 photographs were studied from the minimum of three subjects in each survival time. Additional photomicrographs were taken of specific regions and times when especially active processes of alteration were identified (e.g., 18 hours survival; see also below). Comparable procedures were performed for untreated broodmates. Special attention was given to changes, even subtle alterations in the numerous substructural features, including membranes, organelles, nuclear and cytoplasmic contents, intercellular contacts, and junctions of hair and support cells and their surrounding microenvironment. Hence, we report here a sequence of degenerative changes that is extrapolated from analysis of hundreds of micrographs from closely spaced, early survival times.

RESULTS

Ultrastructure of the control basilar papilla

The structure of the chick basilar papilla has been extensively described by a large number of investigators. Here, for the purpose of relating to our observations on aminoglycoside-treated organs, we reiterate some ultrastructural details. The 3–5-day-old chick basilar papilla is a sickle-shaped structure about 3.8 mm long (Ryals and Rubel, 1982; Ryals et al., 1984) lined by supporting cells and hair cells with stereocilia bundles projecting into the endolymph of the scala media. The hair cells are surrounded by the supporting cells, whose nuclei may be distributed toward the basilar membrane or at midlevels, inferior to the hair cells. The descriptions of the sensory epithelium will be from the area of interest, approximately 400 μm from the basal tip. Sections from the control chick basilar papilla demonstrate relatively consistent findings in hair cells and supporting cell structure during the age range studied. Although there is some variation in fixation, the preservation of the ultrastructure of the hair cells, afferent and efferent terminals, supporting cells, eighth nerve fibers, and other cytoskeletal elements is excellent (Fig. 1A,B). At this level of the papilla, the short hair cells measure approximately 5–7 μm in height and are angular in shape in the more inferior, or abneural, region, whereas more superiorly they are taller (7–9 μm) and often rectangular or elongated. The stereocilia are well preserved, and the tallest stereocilium of each hair cell is contiguous with the tectorial membrane. The tectorial membrane also appears to contact the microvilli of the supporting cell apical surface, separating adjacent hair cells (Fig. 2A,B). The hair cell nuclei are round or oval, with a patchy chromatin pattern and with one or two nucleoli. Euchromatin and heterochromatin patterns are observed among the hair cell nuclei.

Of note is that hair cells demonstrate signs of intensive metabolic activity. The cytoplasm of the hair cells is very dense, owing in part to the presence of numerous polyribosomes embedded in the cytoplasm (Figs. 1B, 2A–D). Rough endoplasmic reticulum is common in the perinuclear region and in the angular extensions near the cuticular plate and surface membrane (Figs. 1B, 2A–C). Smooth endoplasmic reticulum and Golgi formations also are seen in the cytoplasm. Mitochondria are numerous throughout and may show slight variations in size, shape, and electron density (Figs. 1B, 2A,C,D). Inclusion bodies are seen occasionally, but typical lysosomes and phagosomes are infrequent. Some vesicles and vacuolar structures can be seen in different regions of the cytoplasm and are often clustered at the basal or basolateral region of the hair cells (Fig. 1B). Filaments of various types are observed as well as microtubules. The filamentous substructure is particularly evident at the specialized junctions between hair cells and support cells (Fig. 2A,B). At the lumenal surface, two and sometimes three specialized junctions occur between all hair cell–supporting cell contacts. Tight junctions, or zonulae occludens, face the lumen. Zonulae adherens are below the tight junction, and

Fig. 2. **A:** Electron micrograph of normal supporting cell (SC) processes separating two hair cells (HC) to show junctions (arrows) between SCs and HCs and the gap junctions (circles) between adjacent SCs only. Normal intercellular space (arrowheads) occurs only between SCs and HCs, whereas the gap junctions are extensive and occur only between SCs throughout the basilar papilla. On these middle-range magnifications, the gap junctions appear as very dense, closely applied membranes in contrast to the usual intercellular spacing (compare arrowheads with circled gap junctions). The hair cell cytoplasm is characterized by dense arrays of polyribosomes (r) and interspersed normal mitochondria (M). LU is lumen or scala media, and strands from the tectorial membrane (t) are contiguous with the SC microvilli (m). **B:** Higher magnification of a normal single supporting cell (SC) process with microvilli (m) to show the tight junctions (zonulae occludens, arrowhead) and the zonulae adherens (arrows) junctions that always appear between the SCs and the adjacent hair cells (HC). The third type of junction, macula adherens or desmosome, may also be seen here in some sections. The lucent cytoplasm of the SC is contrasted with the dense, granular, ribosome-rich (r) cytoplasm of the hair cell. A "vestigial" basal body (B) occurs in the SC. **C:** Efferent (E) axon terminal forming a synaptic contact (arrows) onto the basal portion of a normal hair cell (HC). A subsurface cistern (arrowhead) is seen postsynaptically in the hair cell. Support cell (SC) processes with organelle-poor cytoplasm surround the terminal and have gap junctions (circle) with adjacent SCs only. **D:** Afferent (A) terminal making a synaptic contact onto the basal part of a normal hair cell (HC). A presynaptic dense body (arrowhead) surrounded by synaptic vesicles is seen opposite the synaptic cleft and postsynaptic specialization (arrow). Scale bars = 1 μm.

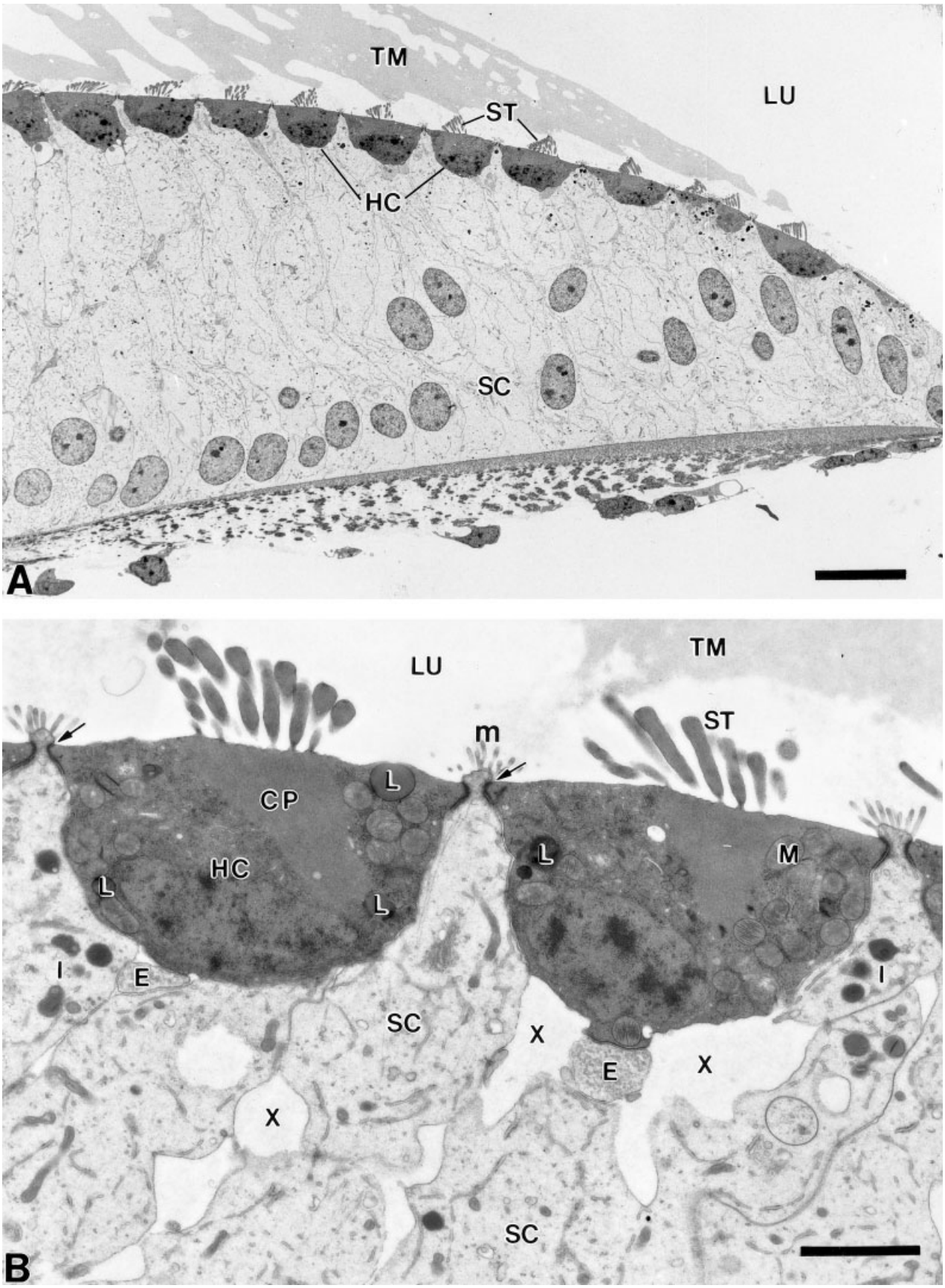

Figure 3

beneath this the maculae adherens, or desmosome, are observed in some sections. No gap junctions could be identified between hair cells and supporting cells, but they are common between adjacent supporting cells throughout the basilar papilla (Fig. 2A).

The synaptic patterns of the basilar papilla are thoroughly described in the literature (Takasaka and Smith, 1971; Hirokawa, 1978; Rebillard and Pujol, 1983; Whitehead and Morest, 1985) and consist of classical afferent and efferent terminals that form contacts on the basal and basolateral surfaces of hair cells. The organ-supporting cells rarely receive synaptic contact; however, Oesterle and colleagues (1992) have shown efferent synapses on hyaline cells that lie at the extreme inferior region (lateral to the sensory epithelium) and are also seen here. Efferents onto hair cells are 1–3 μm bulb-shaped axon terminals filled with round and pleomorphic synaptic vesicles that form presynaptic contacts at a membrane specialization (Figs. 1B, 2C). These terminals are often apposed by a subsynaptic cisterna in the hair cell cytoplasm immediately opposite the aggregated synaptic vesicles in the active zone of the presynaptic terminal (Fig. 2C). They are more frequent on short hair cells, often with two or more terminal synaptic profiles per hair cell profile, but may also occur singly on some taller hair cell profiles. Afferent dendritic terminals synapse mainly on taller hair cells and are either small (1–3 μm) and knob-shaped (Fig. 1B) or extensive, elongated processes (3–4 μm) abutting the tallest, most superior hair cell profiles (a portion of one is shown in Fig. 2D). They have few pleomorphic vesicles, vacuoles, or organelles, and they are often opposite synaptic bodies, decorated with round synaptic vesicles in the hair cell cytoplasm (Fig. 2D).

The organ-supporting cells span the basilar papilla, resting basally on a basement membrane and emerging apically as a narrow (1 μm) extension between hair cells at the lumen (Figs. 1A,B, 2A,B). They have microvilli at the lumenal surface that often appear contiguous with filamentous strands of the tectorial membrane (Figs. 1B, 2A,B). The relatively electron-lucent cytoplasm contains all of the usual organelles: mitochondria, polyribosomes, glycogen, smooth and granular endoplasmic reticulum, Golgi apparatus, and microtubules and filaments of various sizes, but in sparse quantities compared with those in the adjacent hair cells (Figs. 1B, 2A,B). The finely granular nucleus is often located in the basal region of the cell but occasionally resides at middle levels (Fig. 1A). Inclusion bodies such as phagosomes and lysosomes are present but not numerous in the control material. In addition to the relatively lucent organ-supporting cells, border and hyaline cells are located in the abneural portion of the basilar papilla and contain unique structural features (Oesterle et al., 1992).

Ultrastructure of the aminoglycoside-exposed basilar papilla

We detected some variability in the timing of the observed changes. Therefore, to allow for this overlap of cytological patterns and to provide the orderly sequence of events we observed, we will describe the findings in three groups of 6-hour intervals: early (6–12 hours), middle (12–18 hours), and late (18–24 hours) degeneration times.

Early degeneration: 6–12 hours. The earliest changes we observed occurred at or soon after 6 hours postinjection. They were subtle and variable. However, the structures described above are clearly and reproducibly altered compared with the basilar papillae of control subjects. The earliest, most consistent finding is a change in the shape of the hair cell (Fig. 3A). At all magnifications, it is evident that the hair cell is swollen. However, the apical portions do not protrude into the lumen. Specifically, the basal and lateral surfaces now appear more rounded than the angular shape normally observed in control papillae in the same region (cf. Fig. 3A,B vs. Fig. 1A,B). This is most obvious in the short and intermediate hair cells, whereas the superiorly positioned, taller hair cells undergo milder degrees of swelling (Fig. 4A). There is also increased extracellular space around the hair cells, possibly because of shrinkage of adjacent supporting cells or because of extravasation of fluid into the extracellular space of the sensory epithelium (Fig. 3B).

As early as 12 hours, mitochondrial swelling is apparent in some specimens (Fig. 3B), particularly those with obvious swelling of the cell body. These usually mildly dense but delicate organelles with normal membrane architecture (Fig. 2A,C) now appear as pale and dilated, with compressed cristae (Fig. 3B). Modest nuclear changes, such as early chromatin condensation, consistent with an apoptotic-like process, are seen by 12 hours (not shown) but are more pronounced at slightly later times (see below).

An increase in the number of inclusion bodies, such as different types of lysosome, is also a very early event that can be observed in hair cells as soon as 6–8 hours after drug exposure (cf. Figs. 3B, 4A vs. Fig. 1B). During this time, the short and intermediate hair cells display lysosomes that appear variable in size, 0.2–0.5 μm, and relatively electron lucent or homogeneous. Within hair cells, these inclusions are distributed in a perinuclear pattern in the base as well as in the lateral recesses of the cell. Although these lysosomes also appear to accumulate in tall hair cells, the latter seem to contain variable numbers of denser or heterogeneous-appearing inclusions and lysosomes (Fig. 4A). We did not detect engulfment vacuoles at the subsurface areas or presence of pinocytotic vesicles or phagosomes especially adjacent to the plasmalemma at any level during the first 12 hours. Thus, we cannot definitively conclude whether the lysosomes are the result of an active pinocytotic or phagocytic process or represent autophagy. Shortly after their appearance, most of the inclusion bodies have a uniform, near homogeneous character in many of the hair cells, whereas, later in the

Fig. 3. **A:** Eight hours after a single injection of gentamicin. Several of the hair cells (HC) are rounded and swollen compared with the controls (see Fig. 1A). The stereocilia (ST) and attached tectorial membrane (TM) are unaltered, and the deep-lying support cells (SC) appear normal. LU, lumen. **B:** Twelve hours after a single gentamicin injection. Hair cells (HC) from the inferior to middle region of the papilla show swelling and are rounded but not protruding into the lumen (LU). The stereocilia (ST) appear unaltered, as do the cuticular plates (CP), but the cytoplasm contains slightly dilated mitochondria (M) and homogeneous-appearing inclusions or lysosomes (L). Normal-appearing efferents (E) are seen at the bases of the hair cells, and there is increased extracellular space (X). Supporting cells (SC) maintain the surface junctions with the HCs (arrows) but now seem to contain more inclusions or lysosomes (I) than usually seen in controls. Scale bars = 10 μm in A, 2 μm in B.

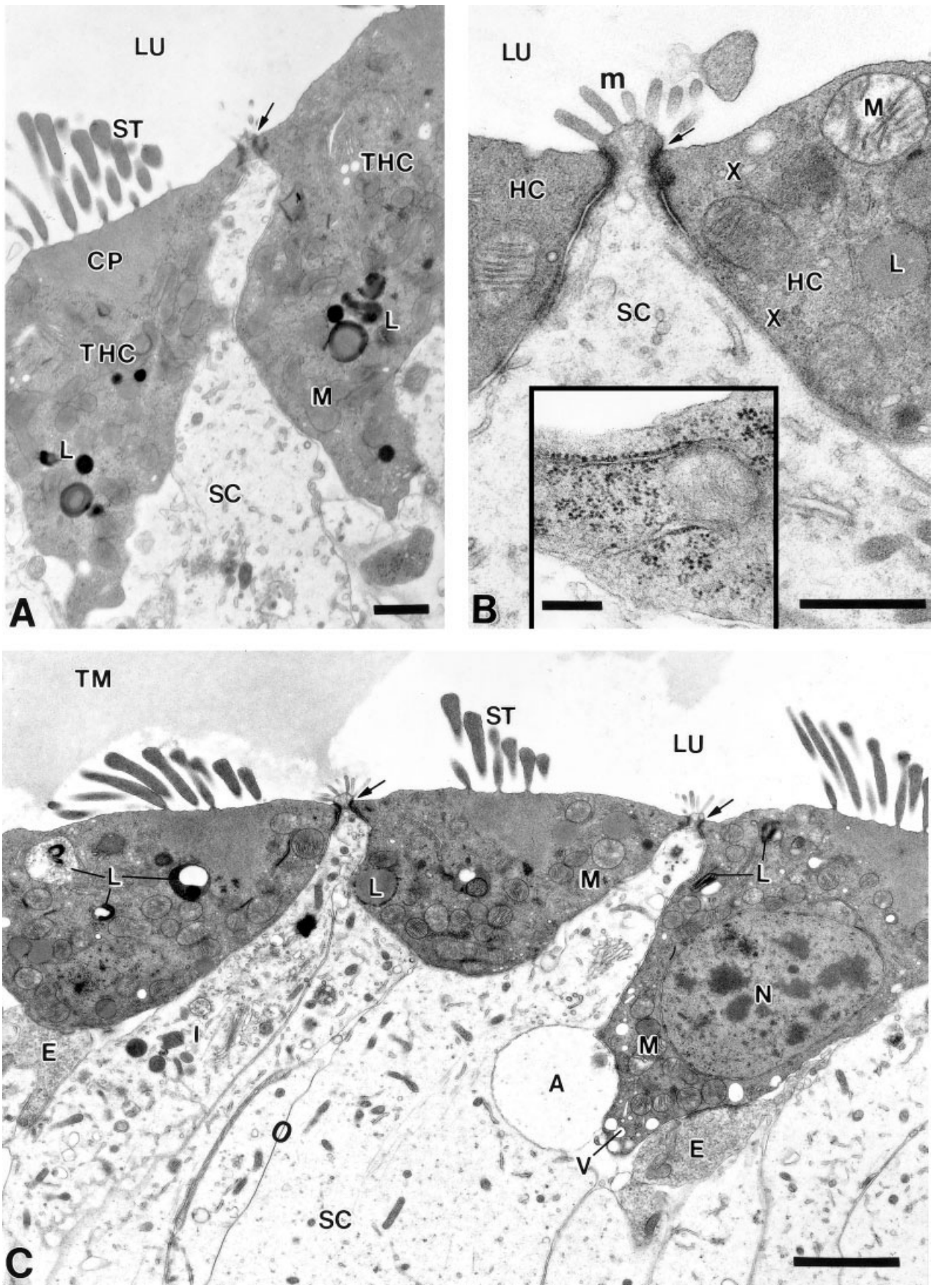
LU
ST
THC
CP
L
THC
M
L
SC
A
LU
m
M
HC
X
L
HC
SC
X
B
TM
ST
LU
L
L
M
L
N
E
I
M
A
O
V
E
SC
C

Figure 4

degenerative process, the lysosomes become more pleomorphic, heterogeneous, and dense.

The supporting cells also accumulate inclusion bodies that resemble lysosomes and are more numerous than in the control tissue, which is interesting. These lysosomes are similar to those in the hair cells, except that they are more electron dense (Fig. 3B). The moderate increase in lysosomes in the supporting cells seems to be concentrated at the lumenal surface of the cells either subjacent to the microvilli or adjacent to the affected hair cells. Although these may represent endocytotic elements from gentamicin or phagocytosis of degenerative debris, structural evidence of such activity on the cell surfaces could not be identified. Subsequent processing of these inclusions or lysosomes may be different in the hair cells.

At this stage, the vast majority of afferent and efferent terminals does not demonstrate any remarkable changes, although a small proportion of the afferents appears to show slight swelling and occasional disrupted surface membranes (not shown). The efferent axons do not appear to be affected. The eighth nerve fibers entering through the habenula perforata are normal appearing without obvious signs of direct toxicity from the drug. The lumenal cell-to-cell contacts between supporting cells and between hair cells and supporting cells are intact without evidence of alteration (Fig. 3A,B). The apical surface specializations including stereocilia and cuticular plates of the hair cells and the microvilli of supporting cells are unaltered. The same is true for the nuclei of both cell types (Fig. 3A,B).

Mid-degeneration: 12–18 hours. During the next 6-hour interval, several overlapping, rapid changes occur, resulting in the first hair cell extrusion (as in Fig. 5A). The short and intermediate hair cells continue to swell and are clearly rounded (Figs. 3B, 4C). Within the hair cells, numerous organelles undergo extensive degenerative transformation (Fig. 4B,C). The polyribosomes that are so prominent in control hair cells undergo dispersion or dissolution, resulting in loss of the characteristic rosettes and the formation of dust-like patches of granular material (Fig. 4B; also compare with Figs. 2A,B and 4B, inset). The region of the hair cell that appears most affected by this ribosomal transformation is the apical area adjacent and subjacent to the cuticular plate.

A further alteration affects many, but not all, of the mitochondria. A greater proportion of these organelles now clearly show variable degrees of dilatation and swelling beyond that seen in any of the controls (Fig. 4B,C). The mildest degree of mitochondrial swelling is detectable by 12 hours, but, by 18 hours, this alteration is much more pronounced and widespread (Fig. 4B,C). Early nuclear alterations, such as chromatin condensation observed at 6–12 hours, are far more obvious and occur in more hair cells than at earlier time points (Fig. 4C). These changes are consistent with descriptions of apoptotic-like degeneration.

As seen above, at 6–12 hours after drug exposure, most of the lysosomes are homogeneously granular and relatively lucent. By 12 hours, some of the taller hair cells show denser, more heterogeneous, and more pleomorphic forms of lysosomes (Fig. 4A). At 18 hours, a larger proportion of the hair cells contains lysosomes at various stages of formation. The homogeneous inclusions or lysosomal bodies observed at earlier time points appear to condense, to become more electron opaque, and to shrink in size (Fig. 5A). Thus, a wide range of pleomorphic-appearing lysosomes occurs in individual hair cells. The lysosomes within the supporting cells are less pleomorphic in appearance.

Clear signs of degenerative changes are apparent in the afferent terminals by 15 hours after exposure to gentamicin (Fig. 4C). Whereas modest swelling or membrane disruption is rarely observed in the afferent terminals of normal and control tissue (Fig. 1B), the drug-treated animals by 18 hours consistently demonstrate severe degrees of swelling and surface membrane lysis as well as deterioration of the internal organelles of most of the afferent terminals (Fig. 4C). The efferent terminals typically remain intact and retain their specialized contacts onto the altered hair cells (Fig. 4C). Infrequently, undamaged efferent terminals may be retracted off the altered hair cells. As the hair cells degenerate and the extrusion process proceeds, apparently unaltered efferent terminals can be identified deeper in the sensory epithelium (Fig. 5B; also as in Fig. 5C) with a few afferent terminals, which are often swollen. Some of these vesicle-filled profiles are presumably efferent axon endings retracted from the extruded hair cells. The terminals contain numerous synaptic vesicles and mitochondria, and the surface membrane shows little evidence of disruption in these efferent terminal axons, in contrast to the swollen and retracted afferent terminals. In addition, an occasional efferent terminal attached to an extruded hair cell can be seen in the lumen (as in Fig. 5C, inset).

The first hair cell extrusion from the sensory epithelium consistently appears to be from among the taller hair cells in the most superior or neural regions (Fig. 5A) rather than the intermediate or short hair cells located more inferiorly. The hair cells adjacent to extruded ones show a greater amount of lumenal blebbing (as in Fig. 5C). They are not as swollen as the short hair cells but are more scalloped or shrunken, and they contain larger numbers of dense, fragmented inclusion bodies and lysosomes than do

Fig. 4. **A:** Same material as in Figure 3B to show the superiorly occurring taller hair cells (THC), with increased numbers of dense inclusions or lysosomes (L) and only modest dilation of the mitochondria (M). Swelling is not as evident as in the short hair cells, but these cells appear to be shrunken and denser than in normals. Stereocilia (ST) and cuticular plates (CP) are intact, the former not showing fusion. Supporting cells (SC) retain normal junctions (arrow) with the hair cells at the lumen (LU). **B:** Higher magnification micrograph from a preparation 18 hours after gentamicin injection. Mitochondria (M) show advanced swelling, and lysosomes (L) are evident. The polyribosomes are greatly reduced or lost compared with controls (compare with Figure 2A and inset), and patches of so-called ribosomal "dust" (x) are seen. The supporting cell (SC) retains normal-appearing junctions (arrow) with the hair cells (HC) and has usual microvilli (m) at the lumen (LU). **Inset:** A portion of a normal (control) hair cell at comparable magnification (as in Fig. 2A,B) to illustrate a normal pattern of polyribosomes that seem to have been lysed in the gentamicin-treated preparations. **C:** Fifteen hours after gentamicin injection. Hair cells show swelling and distortion with dilated mitochondria (M), vacuoles (V) and lysosomes (L) of various types from homogeneous to complex ones. The nucleus (N) also shows chromatin dispersion. A disrupted afferent ending (A) and normal-appearing efferent endings (E) are seen. Stereocilia bundles (ST) and cuticular plates are intact. Support cells (SC) have numerous and extensive gap junctions (circle) again and normal-appearing surface junctions (arrows) with adjacent hair cells. They also contain several inclusion bodies (I). Scale bar = 1 μm in A,B, 2 μm in C, 0.5 μm in inset.

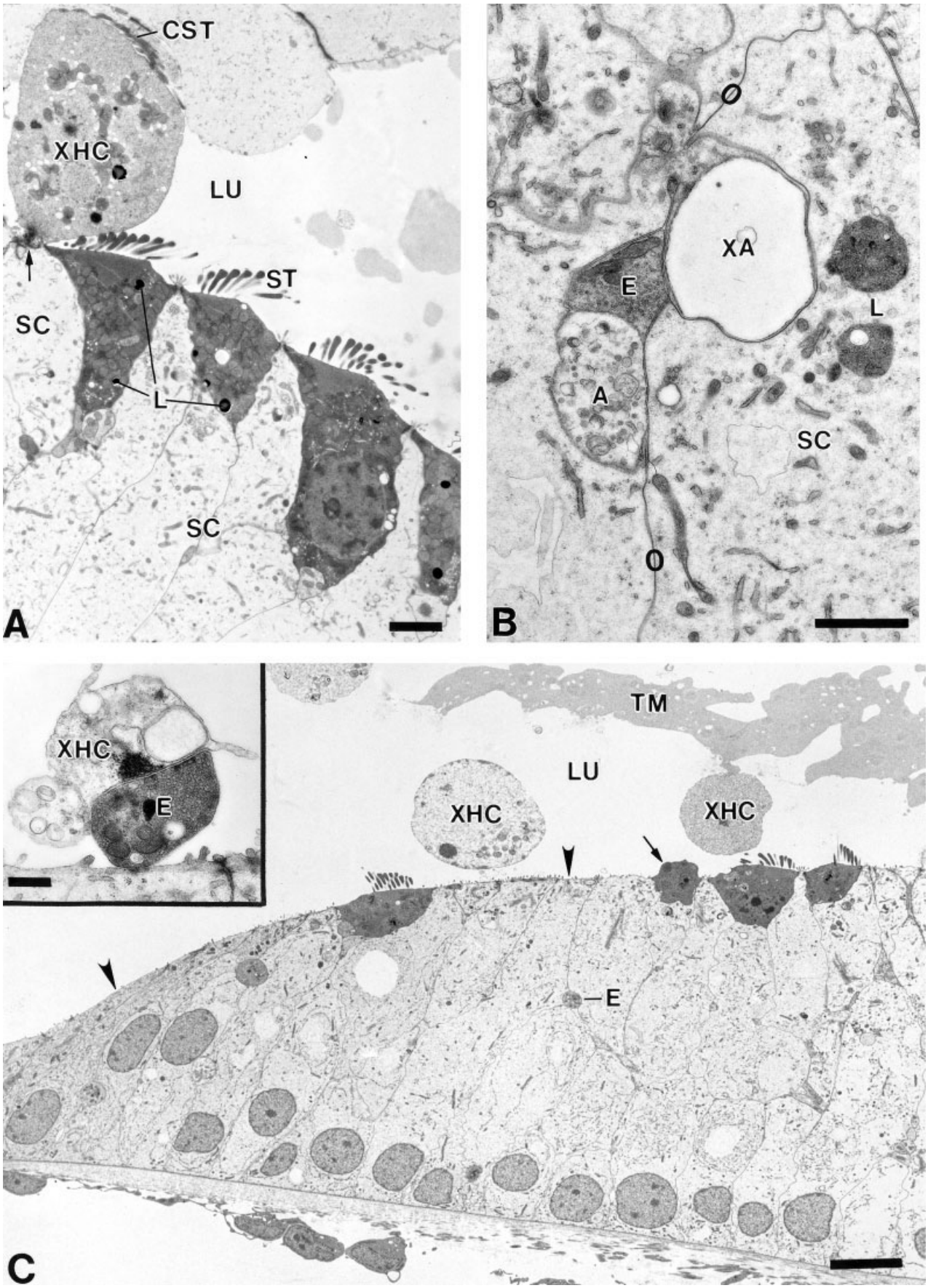

Figure 5

the shorter ones (Fig. 5A). However, there is little to suggest that tall cells would be more susceptible than short hair cells to the drug-induced damage. It appears that, just prior to hair cell extrusion, the shorter hair cells swell and become electron lucent, whereas the tall hair cells shrink and condense.

Late degeneration: 18–24 hours. During the period from 18 to 24 hours after gentamicin injection, rampant extrusion of hair cells occurs throughout the width of the epithelium at this level of the papilla (Fig. 5C). Ten or more extruded hair cells may be seen in a single ultrathin section. Extrusion is sometimes preceded by cytoplasmic blebbing, which involves the entire apical/lumenal surface of the hair cell (Fig. 5C). The extrusion process of the hair cell includes the stereocilia, the cuticular plate, the underlying cytoplasm, and the accompanying organelles. Small buds of cytoplasm and plasma membrane are also seen emerging beyond the apical surface, but these are not nearly as impressive as those cells in the process of active extrusion. While the altered hair cells are in the process of being ejected, the supporting cell lumenal surface expands and enlarges, extending beneath and displacing the emerging degenerated hair cell into the lumen (Fig. 6A,C). Throughout the process of hair cell extrusion, the supporting cells maintain their usual gap junctions complexes with their neighboring supporting cells below the extruding hair cell (Fig. 6C).

During the entire process of extrusion, the tight and adherens junctions between the hair cells and the supporting cells remain intact (Fig. 6A,C). Furthermore, the surface membrane of the degenerated and extruded hair cells shows only occasional rupture along with the tremendous degree of cellular swelling (Fig. 6A–C). While the hair cells are being ejected, the tight junctions appear to contract around the hair cell until only a small segment of this contact remains (Figs. 6A,C, 7B). These tight junctions persist until the hair cell is completely ejected into the endolymph. Patches of densities are seen on expanded supporting cells at the lumenal surface and presumably are the supporting cell half of the now disconnected tight and adherens junctions with the extruded hair cells. A few examples of these junctions are seen near the time of separation (Fig. 7B).

During the process of hair cell degeneration, some hair cells remain relatively intact (Fig. 6A), whereas others fragment and lose their cellular integrity (Fig. 5C). Hair cell extrusion is a rapid process that results in massive loss of the sensory cells over a large area. Accompanying the obvious cellular loss, there are few, and subtle, intracellular changes that precede the cell's extrusion. For example, these hair cells do not demonstrate stereocilia fusion, and only minimal changes are observed in the cuticular plate. The nuclei are intact with only modest disruption of the nuclear envelope within the extruded cells (Fig. 6A). The usual organelles persist, although the density of polyribosomes is significantly reduced. Some mitochondria appear swollen, whereas others are normal (Fig. 6A,C). At this late stage, lysosomes of various forms are present but are not numerous and do show some disrupted membranes (Fig. 6A,C). Some of the extruded hair cells demonstrate advanced fragmentation and disruption, in particular those that are displaced from the sensory epithelium and appear trapped in the tectorial membrane (Fig. 5C).

Hair cells may occasionally undergo in situ degeneration without being extruded from the sensory epithelium (Fig. 6B). In situ degeneration within the sensory epithelium at this level, however, is by far less common than the process of hair cell extrusion. There are approximately 100 extruded hair cells for each in situ degenerated hair cell. In these cases, the hair cell becomes electron dense, shrunken, and scalloped in shape and is retained within the sensory epithelium, surrounded by expanded supporting cells (Fig. 6B). Nuclear chromatin clumping is common in these cells. There are no signs of blebbing or extrusion, but the electron-dense cell may show fragmentation and phagocytosis by adjacent supporting cells. Nearby supporting cells do have increased amounts of dense inclusions and engulfed debris (Fig. 6B,C).

By 18–24 hours after gentamicin exposure, most of the basilar papillae are denuded of hair cells at the level studied (Fig. 7A). Also, by 24 hours, the afferent terminals of the cochlear ganglion cells are extensively degenerated. They appear swollen, electron lucent, and often devoid of organelles. Expanded mitochondria and a few vacuoles persist. Portions of some terminals appear to have been engulfed within neighboring supporting cells (Fig. 6A). The efferent terminals do not degenerate, even after extrusion of the target hair cells. In fact, normal-appearing, vesicle-filled efferent terminals, without synaptic junctions, can be observed below the expanded supporting cells in areas devoid of hair cells (as in Fig. 5B,C). The neural processes entering through the habenula perforata are intact without signs of degradation at this time, and the cochlear ganglion cells seen at this level also lack evidence of degeneration (not shown).

Fig. 5. **A:** Eighteen hours following gentamicin injection, from the most superior region of the papilla to demonstrate a swollen, extruded hair cell (XHC) still attached (arrow) to the supporting cell process (SC) and with a bundle of collapsed stereocilia (CST). Nearby taller hair cells show shrinkage, increased density, and several dark lysosomal inclusions (L) but normal-appearing stereocilia (ST). LU, lumen. **B:** Eighteen hours after a single gentamicin injection subjacent to the lumenal surface to show an example of normal-appearing afferent (A) and especially efferent (E) terminals, the latter filled with the usual synaptic vesicles but lacking synaptic contacts. An example of the numerous swollen or lucent, presumed afferent (XA) terminals that occur among the supporting cell processes (SC) is also shown. Lysosomes (L) or inclusion bodies are seen within many of the SCs. Gap junctions (circles) between the SCs are also extensive. **C:** Twenty-one hours following gentamicin injection. Low-power view of a papilla showing several extruded hair cells (XHC) in various stages of advanced degeneration, some of which appear attached to the tectorial membrane (TM). Large areas of the papilla are devoid of hair cells (arrowheads), but some of those remaining appear swollen or protruding (arrow) into the lumen (LU). **Inset:** From a comparable preparation illustrating a fragment of an extruded hair cell (XHC) with an attached vesicle-filled presumed efferent terminal (E). The supporting cells are at the bottom. Scale bar = 2 μm in A; 1 μm in B and inset; 10 μm in C.

DISCUSSION

In summary, the first 24 hours after a single high-dose injection of gentamicin yields rapid extrusion of the majority of hair cells in the basal region basilar papilla. The complete loss of hair cells in the region studied, about 400 μm from the basal tip, is a function of the high dose of gentamicin used in this study and the location along the basilar papilla. This location has previously been noted to

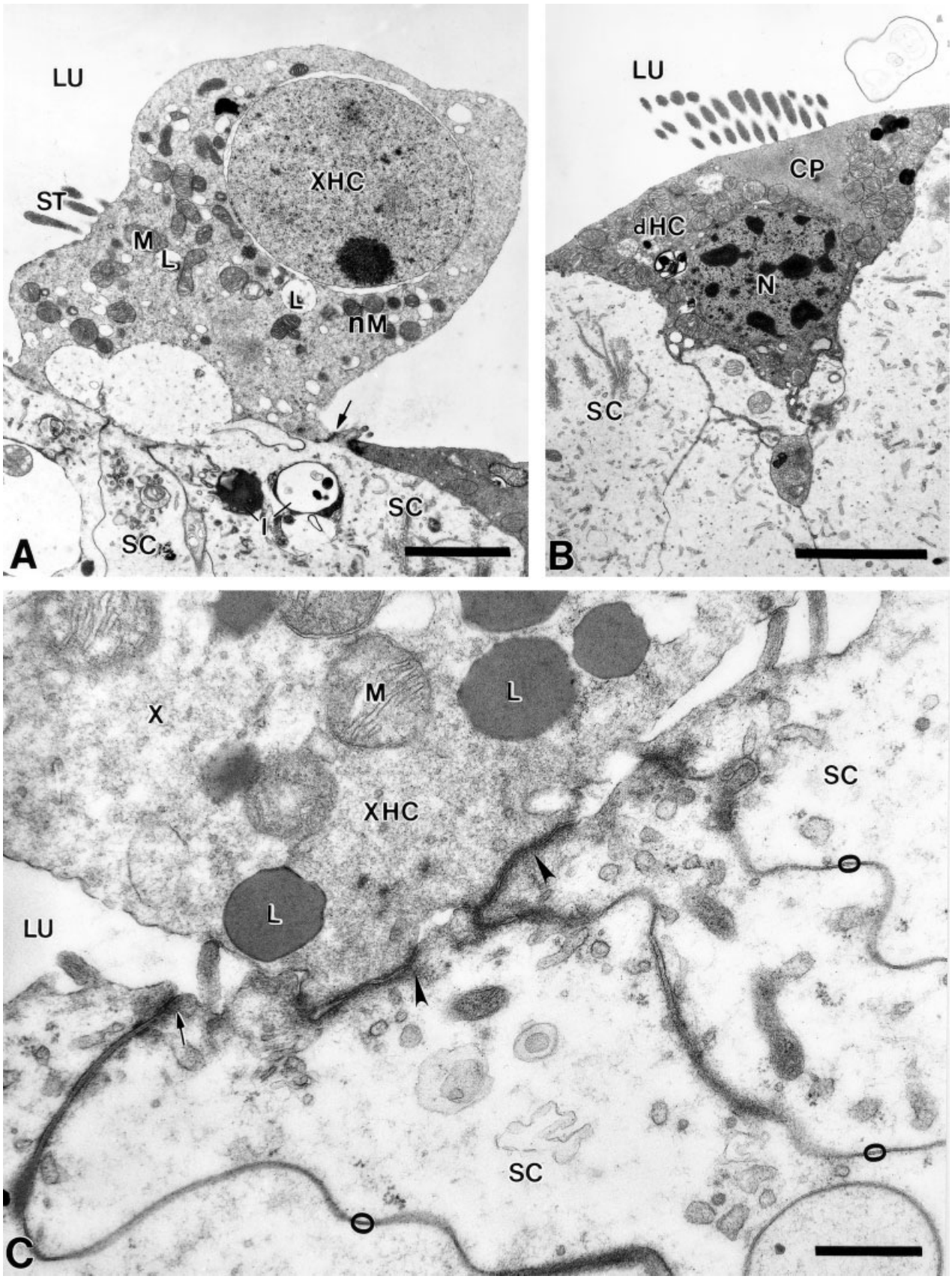

Figure 6

be in the middle of the damaged region after gentamicin exposure (Janas et al., 1995; Stone et al., 1996). It is important to note that the extent of damage depends on the age of the animal as well as dosage, type of aminoglycoside, and administration schedule (see Cotanche, 1999). The earliest ultrastructural changes, seen in our material at 6–12 hours postinjection, include rounding of the subluminal portion and swelling of the short hair cells, dilatation and disorganization of some of the mitochondria, and formation of inclusion bodies or lysosomes, which progress from a pale, homogeneous, electron-lucent appearance to a heterogeneous, dark, condensed appearance at later times. At the middle time points, 12–18 hours postinjection, characteristic findings consist of afferent terminal swelling and lysis, polyribosomal dispersion or dissolution, and extrusion of the taller hair cells toward the superior border. In the later stages of this study, 18–24 hours after gentamicin injection, there was evidence of rampant hair cell extrusion, expansion of the apical surface of the supporting cells, and preservation of the efferent terminals, which appear to remain present within the supporting cell layer.

The process of hair cell death in the avian basilar papilla bears some resemblance to features of classic apoptosis, but the extrusion process may be quite unique. The in situ degenerated hair cells do fit the classic description of the apoptosis, in that the cell shrinks and darkens, the nucleus condenses and fragments, and the cell contents are phagocytosed by neighboring cells without compromise of the plasma membrane. However, the majority of cells die by the extrusion process, which may be characteristic of apoptotic events in which it is important to maintain an epithelial barrier (Rosenblatt et al., 2001). These two types of hair cell death have been systematically studied and described in the mammalian vestibular system, and the cellular changes observed after aminoglycoside exposure in the guinea pig utricle are nearly identical to what we have observed here in the avian basilar papilla (Li et al., 1995).

It is possible that some of the early changes described for apoptotic pathways do occur in the extruded cells, but they cannot be observed with electron microscopy. Activation of caspases 8 and 9 and protection of hair cells with inhibition of caspase activity have been observed in both cultured avian papilla and murine utricle after aminoglycoside exposure (Forge and Li, 2000; Cunningham et al., 2002; Cheng et al., 2003). Although caspase activation may point toward an apoptotic mechanism of cell death (see also Torchinsky et al., 1999), this caspase activity has not been correlated with any morphologic ultrastructural changes that could be observed in this study, nor was an apoptotic-like pathway directly supported or refuted by the ultrastructural findings in vivo. Given that there is a continuum between apoptotic and necrotic characteristics of cell death and that distinctions between the two may be blurred in some cases, the specific features of cellular degeneration are potentially important observations for providing insight into the mechanism of aminoglycoside ototoxicity and possibly other challenges that result in hair cell death, even if they do not conform to classic descriptions of either necrosis or apoptosis (Bursch et al., 2000; Martin, 2001).

During the process of hair cell degeneration, there was never evidence of violation of the reticular lamina. The hair cells appear to be evacuated from the sensory epithelium with such speed that most hair cells are observed floating in the scala media, relatively intact. The hair cells that degenerate in situ, by far in the minority, undergo phagocytosis by the adjacent supporting cells without any resultant compromise in the reticular lamina as well. During the period of extrusion and phagocytosis, the supporting cells retain the tight junctions and adherens complexes necessary to maintain a strict separation between perilymph and endolymph that allows for preservation of the endocochlear potential and thereby allows the undamaged portion of the organ to continue functioning.

Some of the oldest studies on hair cell ultrastructure after aminoglycoside exposure revealed that certain organelles were targeted by the aminoglycoside. In 1962, Wersäll and Hawkins described the effect of streptomycin on the cat vestibular hair cells and noted some findings similar to what we observe in the chick. They noted formation of dark "osmiophilic bodies," presumably similar to the lysosomes that we saw; degeneration of mitochondria; and formation of myelin figures. The "protoplasmic protrusions" of the cytoplasm described by them appear to resemble cytoplasmic blebs that we occasionally witnessed prior to extrusion of hair cells. This group also described mitochondrial pathology in the lizard vestibular organs after systemic gentamicin administration (Bagger-Sjoback and Wersäll, 1978). The observations were similar to what was described in cat: large swollen mitochondria and dark condensed mitochondria with lamellar structures described as myelin bodies. Ryan and colleagues (1980) described electron microscopic observations of surviving hair cells following kanamycin injections in chinchilla. Outer hair cells were preferentially damaged, some of the afferent terminals were atrophic, and the efferent fibers were damaged in the regions of outer hair cell damage. Examination of surviving hair cells revealed increased lysosomes, the disarrayed mitochondria, and the blebbing of the cuticular plate or extrusion of hair cell cytoplasm. Therefore, despite the fact that these tissues were subjected to repeated doses of drug and the fact that these were chronically deafened animals (2–6 weeks after drug exposure), the findings reported in earlier studies are very similar to what we describe here.

Fig. 6. **A:** Example of a swollen, extruded, and degenerated hair cell (XHC) extending into the lumen (LU) at 18 hours of survival. It still retains attachments (arrow) with the subjacent supporting cell processes (SC), which themselves contain inclusions (I). The extruded cell has mitochondria that are swollen (M) and others that are normal-appearing (nM). Several lysosomal inclusions (L), a finely granular cytoplasm, and a nucleus with an enlarged envelope can also be seen. A few stereocilia (ST) can be seen, but the cuticular plate is not present in this plane of section. **B:** Example of a dense hair cell (dHC) presumably degenerating "in situ" at 24 hours of survival. Contrast this with the far more commonly occurring swollen, extruded hair cell shown in A and in Figure 2A,B. A shrunken cuticular plate (CP) and a nucleus (N) with chromatin condensation are seen. LU, lumen; SC, supporting cell process. **C:** Example of the interface between support cell processes (SC) and a degenerating hair cell (XHC) during the final process of extrusion, seen by 18 hours of survival. Junctional complexes (arrowheads) are seen with portions of the extruded hair cell still attached at some of these sites. A tight junction is seen between SCs (arrow), and extensive gap junctions also occur (circles). The XHC shows several lysosomes (L), mitochondria (M), and a cytoplasm that is devoid of the usual compliment of ribosomes but appears finely granular (X). LU, lumen. Scale bar = 2 μm in A,B, 1 μm in C.

A number of correlations can be made between the histopathologic observations and previous descriptions and hypotheses of the mechanism of gentamicin ototoxicity. In studies using tritiated gentamicin sulfate and electron microscopic immunohistochemistry, these molecules have been localized to the lysosomal compartment of hair cells in both mammals and birds (De Groot et al., 1990; Hashino and Shero, 1995; Hashino et al., 1997). Furthermore, histochemical studies indicate that the uptake of aminoglycoside appears to be concentrated in the basal turn of the mammalian cochlea, which is analogous to the proximal portion of the basilar papilla in birds. The observation of lysosomal formation and subsequent lysosomal degradation during the first 24 hours after gentamicin injection is entirely consistent with the previous reports from aminoglycoside tracer studies. It is postulated by Hashino and coworkers (1997) that hair cell death is caused by leakage of the aminoglycoside from the lysosomal compartment into the cytosol. In this study, the hair cells that contained labeled aminoglycoside in the cytosol were noted to have more significant histopathology than those in which labeling was restricted to the lysosomes. In the current study, the earliest hair cells to be extruded appeared normal prior to extrusion, without significant cytopathic changes. Therefore, it appears possible that extrusion may occur even in the absence of these features described after lysosomal disruption.

The role of mitochondria in aminoglycoside ototoxicity has been extensively studied, both in animals and in humans (Bagger-Sjoback and Wersäll, 1978; Arnold et al., 1981; Hutchin and Cortopassi, 1994, 2000; Fischel-Ghodsian, 1998; Guan et al., 2000; Schleiffer et al., 2000). The rationale for a prominent role of mitochondria in hair cell degeneration is supported by two observations. First, the antimicrobial mechanism of aminoglycoside antibiotics is based on their ability to bind the 12S ribosomal subunit of bacteria, which is analogous to the protein synthesis machinery of the mitochondria in eukaryotic organisms. Thus, it is possible that the mechanism that provides aminoglycoside antibiotics with effective bacteriocidal activity is also responsible for a deleterious effect on eukaryotic mitochondria. The clinical data also support the hypothesis that a mitochondrial abnormality could result in aminoglycoside ototoxicity. Several family pedigrees have been identified in which members with mitochondria abnormalities suffer from being highly vulnerable to aminoglycoside ototoxicity. A recent study using a lymphoblastoid cell line from a patient population with a mitochondrial mutation found that aminoglycoside exposure caused a significant decrease in the rate of mitochondrial protein synthesis, compared with the effect on mitochondrial protein synthesis in cells from their unaffected family members (Guan et al., 2000).

There have been numerous reports of mitochondrial pathology witnessed in hair cells exposed to aminoglycosides (Wersäll and Hawkins, 1962; Bagger-Sjoback and Wersäll, 1978; Leake-Jones et al., 1980; Arnold et al., 1981; Forge, 1985). In the current protocol, morphologic changes in the mitochondria were observed, but the changes did not appear to be the first changes, nor did they appear to be consistent or irreversible. Although a significant number of hair cells demonstrated mitochondrial swelling and disorganization of the cristae at 12–18 hours postinjection, some extruded cells demonstrated mitochondria that appeared relatively healthy. It remains possible that the mitochondria serve to sequester calcium or to buffer pH changes within the cytosol during the early phases of hair cell injury and that, after a certain point, the mitochondria cease to function and thereby regain a more normal-appearing morphology. The fact that, in the extruding cell, some of the mitochondria appear relatively normal does not exclude the possibility that they may be entirely nonfunctional at that point.

Dispersion of the polyribosomes is an early feature in the destruction of the auditory hair cells that has been seen in other forms of cell death. The process of cell death in the primary neurons of the chick cochlear nucleus after deafferentation has been described, and changes in the ultrastructural appearance of ribosomes and immunostaining of Y10B, a monoclonal antibody for ribosomal RNA, were noted (Rubel et al, 1991; Garden et al., 1994; Hartlage-Rübsamen and Rubel, 1996). The degradation of polyribosomes and the subsequent inability to regulate protein synthesis are thought to be a determining step in the fate of these neurons in the process of cell death.

Ultrastructural changes involved in the process of hair cell degeneration after aminoglycoside exposure have been extensively studied in the mammalian vestibular system (Forge, 1985; Li et al., 1995; Forge and Li, 2000). Numerous observations from these studies appear to be similar to what we have observed in the avian basilar papilla. Forge and colleagues describe two types of hair cell loss, degeneration within the epithelium and extrusion from the epithelium. The process of cell death in the avian basilar papilla is nearly identical. The overwhelming majority of auditory hair cells is removed via extrusion, and it is the small minority of hair cells that undergoes the shrinkage, darkening, and nuclear fragmentation characteristic of apoptosis. The hair cells that extrude demonstrate some minor cytopathologic changes, as described above, in the first 12 hours after drug exposure. However, at the time when these cells begin to extrude, they appear largely intact, suggesting that the extrusion process is facilitated by an active process among the supporting cells. The process of extrusion is preceded by cytoplasmic blebbing from the apical surface of the cell membrane, but the cytoplasmic contents do not appear to disrupt the cuticular plate, nor do they necessarily disrupt the structure of the stereocilia. Fusion bundles, which are reported for the auditory hair cells of mammalian species, are not witnessed in the chick basilar papilla (Takumida et al., 1989). Small plasma membrane blebs or protrusions in the control subjects were seen in the previous study of guinea pig vestibular organs. Likewise, for the chick, we occasionally witnessed small cytoplasmic blebs in the control animals; however, they were characteristically present on the side of the hair cell away from the tallest stereocilium, and they did not cause any distortion of the cuticular plate or the stereocilia.

The process of extrusion in this paradigm was also analogous to that described for the vestibular organ, in that the reticular lamina was never violated during the process of hair cell degeneration (Li et al., 1995). During the process of extrusion, the tight junctions that maintain the strict separation between endolymph and perilymph were maintained until the hair cell was released from the final apical attachment to the supporting cell. At various locations and times, numerous hair cells were seen resting on the apical surface of the supporting cells attached only by the last remaining tight junction before they were re-

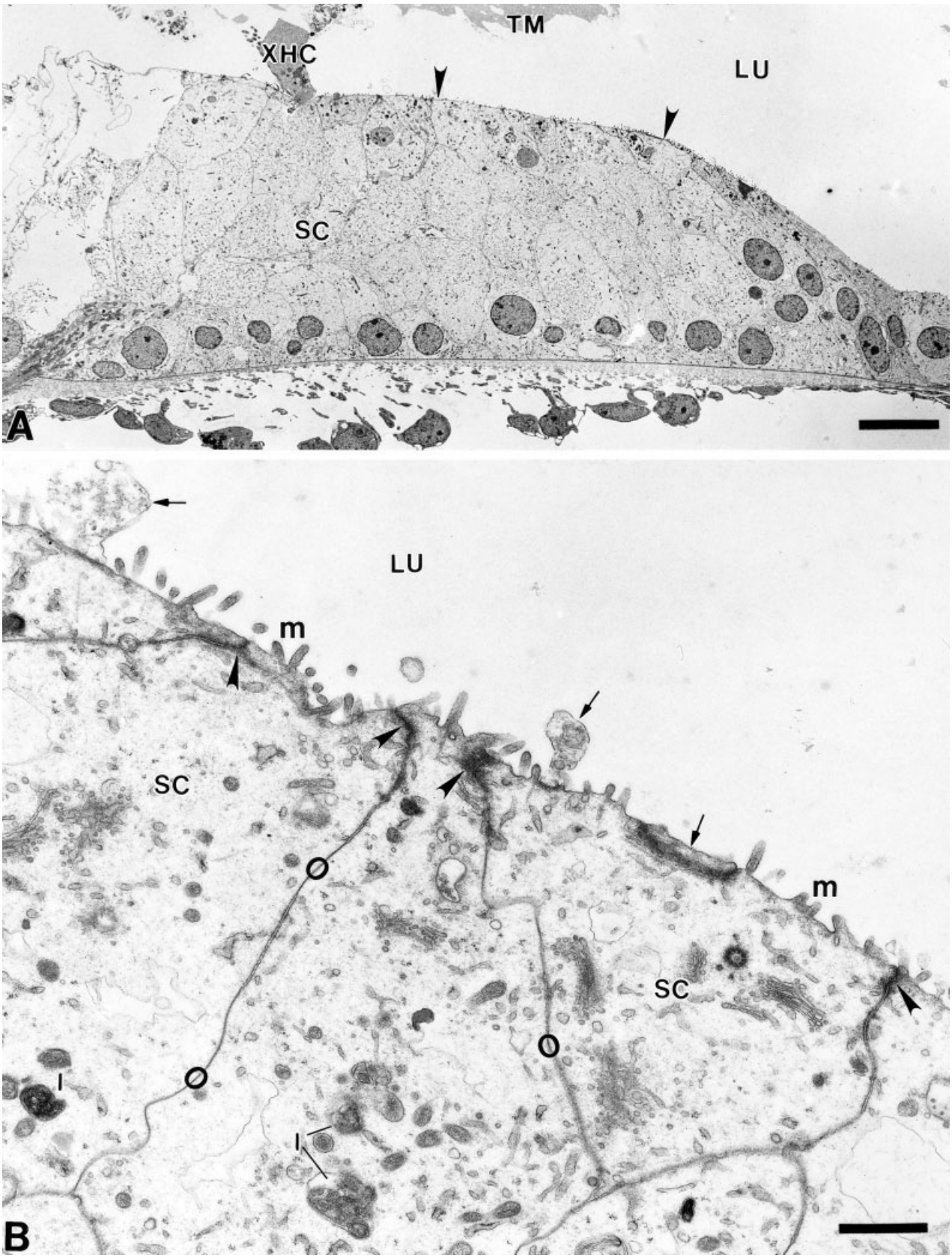

Fig. 7. **A:** By 24 hours, the basilar papillae at this level are essentially devoid of hair cells (arrowheads) and show expansion of the supporting cells (SC). In this particular section, a last dead hair cell (XHC) is being extruded. TM, tectorial membrane; LU, lumen. **B:** Another section at 18 hours of survival, with a broad area devoid of hair cells but with expanded support cell processes (SC) at the lumen (LU). These processes retain normal intercellular junctional complexes (arrowheads) and often have remnants of extruded hair cells (arrows) still attached to them. The numbers of microvilli (m) are obviously reduced on the lumenal surface of the expanded processes. Gap junctions (circles) are seen immediately subjacent to surface. Scale bar = 10 μm in A; 1 μm in B.

leased into the endolymphatic space. Likewise, the hair cells that degenerated in situ with features more characteristic of apoptosis were not witnessed to have any cell membrane breaks or ruptures by 24 hours. The cell underwent shrinkage and subsequent phagocytosis by surrounding support cells, and the fragments of these cells were readily visible in the cytoplasm of these cells.

We also looked for evidence of hair cell repair or an aborted repair process in our tissue. Zheng et al. (1999) provided evidence that some mammalian utricular hair cells lose their stereocilia bundles after exposure to gentamicin in vitro and subsequently resprout the cuticular plate and stereocilia without evidence of cell proliferation or transdifferentiation. Similar conclusions have been drawn from observations on the bullfrog saccule in vitro (Gale et al., 2002). We did not witness any hair cells that underwent partial degeneration, such as loss of the cuticular plate or a pinching off of a blebbed region of the hair cell as has been described in the mammalian vestibular organs. Overall, the process of hair cell degeneration in the high-frequency region of the basilar papilla is characterized by a rapid progression of subtle changes resulting in decisive expulsion of the majority of hair cells and in situ degeneration of the minority of hair cells, leaving the entire sensory epithelium in this region barren of receptor elements within 24 hours of a single dose of gentamicin.

It is conceivable that this organized process of cell extrusion facilitates the advent of supporting cell proliferation and regeneration of new hair cells. During the process of hair cell degeneration, not only is the separation between endolymph and perilymph maintained but, also, efferent terminals remain within the sensory epithelium, with the possibility of providing input to newly developing hair cells. The orderly removal of hair cells via the extrusion process, and the retention of at least a proportion of the neural processes, may facilitate the regeneration of new hair cells. The survival and repair of neural processes and their endings has been extensively studied by Cotanche and colleagues (see Hennig and Cotanche, 1998; Cotanche, 1999), and it appears that the details of survival and regrowth may differ depending on whether damage is induced by intense noise exposure or aminoglycoside treatment.

ACKNOWLEDGEMENTS

Expert editorial assistance was provided by Ms. Laurie Johnson and Ms. Julie Wittges.

LITERATURE CITED

Anniko M, Takada A, Schacht J. 1982. Comparative ototoxicities of gentamicin and netilmicin in three model systems. Am J Otolaryngol 3:422–433.

Arnold W, Nadol JB Jr, Weidauer H. 1981. Ultrastructural histopathology in a case of human ototoxicity due to loop diuretics. Acta Otolaryngol 91:399–414.

Bagger-Sjoback D, Wersäll J. 1978. Gentamicin-induced mitochondrial damage in inner ear sensory cells of the lizard *Calotes versicolor*. Acta Otolaryngol 86:35–51.

Bhave SA, Stone JS, Rubel EW, Coltrera MD. 1995. Cell cycle progression in gentamicin-damaged avian cochleas. J Neurosci 15:4618–4628.

Bursch W, Ellinger A, Gerner C, Frohwein U, Schulte-Hermann R. 2000. Programmed cell death (PCD). Apoptosis, autophagic PCD, or others? Ann N Y Acad Sci 926:1–12.

Chen CS, Saunders JC. 1983. The sensitive period for ototoxicity of kanamycin in mice: morphological evidence. Arch Otorhinolaryngol 238: 217–223.

Cheng AG, Cunningham LL, Rubel EW. 2003. Hair cell death in the avian basilar papilla: characteristics of the *in vitro* model and caspase activation. JARO 4:91–105.

Cotanche DA. 1999. Stuctural recovery from sound and aminoglycoside damage in the avian cochlea. Audiol Neurootol 4:271–285.

Cotanche DA, Saunders JC, Tilney LG. 1987. Hair cell damage produced by acoustic trauma in the chick cochlea. Hear Res 25:267–286.

Cotanche DA, Lee KH, Stone JS, Picard DA. 1994. Hair cell regeneration in the bird cochlea following noise damage or ototoxic drug damage. Anat Embryol 189:1–18.

Cruz RM, Lambert PR, Rubel EW. 1987. Light microscopic evidence of hair cell regeneration after gentamicin toxicity in chick cochlea. Arch Otolaryngol Head Neck Surg 113:1058–1062.

Cunningham LL, Cheng AG, Rubel EW. 2002. Caspase activation in hair cells of the mouse utricle exposed to neomycin. J Neurosci 22:8532–8540.

De Groot JC, Meeuwsen F, Ruizendaal WE, Veldman JE. 1990. Ultrastructural localization of gentamicin in the cochlea. Hear Res 50:35–42.

De Groot JC, Huizing EH, Veldman JE. 1991. Early ultrastructural effects of gentamicin cochleotoxicity. Acta Otolaryngol 111:273–280.

Epstein JE, Cotanche DA. 1995. Secretion of a new basal layer of tectorial membrane following gentamicin-induced hair cell loss. Hear Res 90: 31–43.

Fischel-Ghodsian N. 1998. Mitochondrial mutations and hearing loss: paradigm for mitochondrial genetics. Am J Hum Genet 62:15–19.

Forge A. 1985. Outer hair cell loss and supporting cell expansion following chronic gentamicin treatment. Hear Res 19:171–182.

Forge A, Li L. 2000. Apoptotic death of hair cells in mammalian vestibular sensory epithelia. Hear Res 139:97–115.

Forge A, Schacht J. 2000. Aminoglycoside antibiotics. Audiol Neurootol 5:3–22.

Gale JE, Meyers JR, Periasamy A, Corwin JT. 2002. Survival of bundleless hair cells and subsequent bundle replacement in the bullfrog's saccule. J Neurobiol 50:81–92.

Garden GA, Canady KS, Lurie DI, Bothwell M, Rubel EW. 1994. A biphasic change in ribosomal conformation during transneuronal degeneration is altered by inhibition of mitochondrial, but not cytoplasmic protein synthesis. J Neurosci 14:1994–2008.

Gratacap B, Charachon R, Stoebner P. 1985. Results of an ultrastructural study comparing stria vascularis with organ of Corti in guinea pigs treated with kanamycin. Acta Otolaryngol 99:339–342.

Guan MX, Fischel-Ghodsian N, Attardi G. 2000. A biochemical basis for the inherited susceptibility to aminoglycoside ototoxicity. Hum Mol Genet 9:1787–1793.

Hartlage-Rübsamen M, Rubel EW. 1996. Influence of mitochondrial protein synthesis inhibition on deafferentation-induced ultrastructural changes in nucleus magnocellularis of developing chicks. J Comp Neurol 371:448–460.

Hashino E, Shero M. 1995. Endocytosis of aminoglycoside antibiotics in sensory hair cells. Brain Res 704:135–140.

Hashino E, Shero M, Salvi RJ. 1997. Lysosomal targeting and acculmulation of aminoglycoside antibiotics in sensory hair cells. Hear Res 777: 75–85.

Hayashida T, Nomura Y, Iwamori M, Nagai Y, Kurata T. 1985. Distribution of gentamicin by immunofluorescence in the guinea pig inner ear. Arch Otorhinolaryngol 242:257–264.

Hayashida T, Hiel H, Dulon D, Erre JP, Guilhaume A, Aran JM. 1989. Dynamic changes following combined treatment with gentamicin and ethacrynic acid with and without acoustic stimulation. Cellular uptake and functional correlates. Acta Otolaryngol 108:404–413.

Hennig AK, Cotanche DA. 1998. Regeneration of cochlear efferent nerve terminals after gentamycin damage. J Neurosci 18:3282–3296.

Hirokawa N. 1978. The ultrastructure of the basilar papilla of the chick. J Comp Neurol 181:361–374.

Hirose K, Hockenbery DM, Rubel EW. 1997. Reactive oxygen species in chick hair cells after gentamicin exposure *in vitro*. Hear Res 104:1–14.

Hirose K, Westrum LE, Stone JS, Zirpel L, Rubel EW. 1999. Dynamic studies of ototoxicity in mature avian auditory epithelium. Ann N Y Acad Sci 884:389–409.

Hutchin T, Cortopassi G. 1994. Proposed molecular and cellular mechanism for aminoglycoside ototoxicity. Antimicrob Agents Chemother 38:2517–2520.

Hutchin TP, Cortopassi GA. 2000. Mitochondrial defects and hearing loss. Cell Mol Life Sci 57:1927–1937.

Janas JD, Cotanche DA, Rubel EW. 1995. Avian cochlear hair cell regeneration: stereological analyses of damage and recovery from a single high dose of gentamicin. Hear Res 92:17–29.

Kotecha B, Richardson GP. 1994. Ototoxicity *in vitro*: effects of neomycin, gentamicin, dihydrostreptomycin, amikacin, spectinomycin, neamine, spermine and poly-L-lysine. Hear Res 73:173–184.

Leake PA, Kuntz AL, Moore CM, Chambers PL. 1997. Cochlear pathology induced by aminoglycoside ototoxicity during postnatal maturation in cats. Hear Res 113:117–132.

Leake-Jones PA, O'Reilly BF, Vivion MC. 1980. Neomycin ototoxicity: ultrastructural surface pathology of the organ of Corti. Scan Elec Microsc 3:427–434.

Li L, Neville G, Forge A. 1995. Two modes of hair cell loss from vestibular sensory epithelia of the guinea pig inner ear. J Comp Neurol 355:405–417.

Martin LJ. 2001. Neuronal cell death in nervous system development, disease, and injury [review]. Int J Mol Med 7:455–478.

Matsui JI, Ogilvie JM, Warchol ME. 2002. Inhibition of caspases prevents ototoxic and ongoing hair cell death. J Neurosci 22:1218–1227.

McDowell B, Davies S, Forge A. 1989. The effect of gentamicin-induced hair cell loss on the tight junctions of the reticular lamina. Hear Res 40:221–232.

Oesterle EC, Cunningham DE, Rubel EW. 1992. Ultrastructure of hyaline, border, and vacuole cells in chick inner ear. J Comp Neurol 318:64–82.

Oesterle EC, Tsue TT, Reh TA, Rubel EW. 1993. Hair-cell regeneration in organ cultures of the postnatal chicken inner ear. Hear Res 70:85–108.

Raphael Y. 2002. Cochlear pathology, sensory cell death and regeneration. Br Med Bull 63:25–38.

Rebillard M, Pujol R. 1983. Innervation of the chicken basilar papilla during its development. Acta Otolaryngol 96:379–388.

Roberson DW, Alosi JA, Messana EP, Cotanche DA. 2000. Effect of violation of the labyrinth on the sensory epithelium in chick cochlea. Hear Res 141:155–164.

Rosenblatt J, Raff MC, Cramer LP. 2001. An epithelial cell destined for apoptosis signals its neighbors to extrude it by an actin- and myosin-dependent mechanism. Curr Biol 11:1847–1857.

Rubel EW, Falk PM, Canady KS, Steward O. 1991. A cellular mechanism underlying activity-dependant transneuronal degeneration: rapid but reversible destruction of neuronal ribosomes. Brain Dysfunct 4:55–74.

Ryals BM, Rubel EW. 1982. Patterns of hair cell loss in chick basilar papilla after intense auditory stimulation. Frequency organization. Acta Otolaryngol 93:205–210.

Ryals BM, Creech HB, Rubel EW. 1984. Postnatal changes in the size of the avian cochlear duct. Acta Otolaryngol 98:93–97.

Ryan AF. 2002. Molecular studies of hair cell development and survival. Audiol Neurootol 7:138–140.

Ryan AF, Woolf NK, Bone RC. 1980. Ultrastructural correlates of selective outer hair cell destruction following kanamycin intoxication in the chinchilla. Hear Res 3:335–351.

Schleiffer T, Hart LM, Schurfeld C, Kraatz K, Riemann JF. 2000. Maternally inherited diabetes and deafness (MIDD): unusual occult exocrine pancreatic manifestation in an affected German family. Exp Clin Endocrinol Diabet 108:81–85.

Stone JS, Leano SG, Baker LP, Rubel EW. 1996. Hair cell differentiation in chick cochlear epithelium after aminoglycoside toxicity: *in vivo* and *in vitro* observations. J Neurosci 16:6157–6174.

Takasaka T, Smith CA. 1971. The structure and innervation of the pigeon's basilar papilla. J Ultrastruct Res 35:20–65.

Takumida M, Wersäll J, Bagger-Sjoback D. 1989. Sensory hair fusion and glycocalyx changes after gentamicin exposure in the guinea pig. Acta Otolarngol Suppl 457:78–82.

Torchinsky C, Messana EP, Arsura M, Cotanche DA. 1999. Regulation of p27Kip1 during gentamicin mediated hair call death. J Neurocytol 28:913–924.

Umemoto M, Sakagami M, Ashida K, Fukazawa K, Kubo T, Senda T. 1994. Fine structure aspects on auditory hair cell degeneration in the budgerigar, *Melopsittacus undulatus*, as induced by kanamycin. Arch Histol Cytol 57:395–403.

Wersäll J, Hawkins JE. 1962. The vestibular sensory epithelia in cat labyrinth and their reactions in chronic streptomycin intoxication. Acta Otolaryngol 54:1–23.

Westrum LE, Cunningham DE, Rubel EW. 1998. Electron microscopy of early changes in the avian basilar papilla following gentamicin ototoxicity. Assoc Res Otolaryngol Abs 21: 629.

Whitehead MC, Morest DK. 1985. The development of innervation patterns in the avian cochlea. Neuroscience 14:255–276.

Zheng JL, Keller G, Gao WQ. 1999. Immunocytochemical and morphological evidence for intracellular self-repair as an important contributor to mammalian hair cell recovery. J Neurosci 19:2161–2170.